



Search for Pair-Production of Second-Generation Leptoquarks in $p\bar{p}$ Collisions with the DØ Run II Detector

The DØ Collaboration
URL <http://www-d0.fnal.gov>
(Dated: June 17, 2005)

We report on the preliminary results from the search for second-generation leptoquarks (LQ_2) in $p\bar{p}$ collisions at a center-of-mass energy of $\sqrt{s} = 1.96$ TeV using an integrated luminosity of $(294 \pm 19) \text{ pb}^{-1}$. Since no evidence for leptoquark signal in the $\mu j + \bar{\mu} j$ channel has been observed, upper bounds to the product of cross section times branching fraction $\beta = \text{Bf}(LQ_2 \rightarrow \mu j)$ into a quark and a muon were calculated for scalar second-generation leptoquarks. This yields a lower mass limit of $m_{LQ_2} > 247$ GeV for $\beta = 1$ and $m_{LQ_2} > 182$ GeV for $\beta = 1/2$. Combining these limits with previous results from DØ Run I, the lower limits on the mass of scalar second-generation leptoquarks are $m_{LQ_2} > 251$ GeV and $m_{LQ_2} > 204$ GeV for $\beta = 1$ and $\beta = 1/2$, respectively.

The observed symmetry in the spectrum of elementary particles between leptons and quarks motivates the existence of leptoquarks [1]. Leptoquarks are bosons carrying both quark and lepton quantum numbers and fractional electric charge. Leptoquarks could in principle decay into any combination of a lepton and a quark. Experimental limits on lepton number violations, on flavor-changing neutral currents and on proton decay, however, lead to the assumption that there would be three different generations of leptoquarks. Each of these leptoquark generations couples to one quark and one lepton generation only and, therefore, individually conserves the family lepton numbers. [2]

While the cross section for the single leptoquark production also depends on the a-priori unknown leptoquark-lepton-quark coupling, the production of pairs of scalar leptoquarks only depend on the leptoquark mass.

This analysis focuses on the search for pair-produced second generation leptoquarks (LQ_2). Assuming 100% branching fraction to a charged lepton and a quark, $\beta = BF(LQ_2 \rightarrow \mu j) = 1$, a pair of second-generation leptoquarks, $LQ_2\bar{L}Q_2$, decays into two highly energetic muons and two highly energetic jets with no or little missing transverse energy.

The $D\bar{O}$ detector consists of several layered elements. First, is a magnetic central-tracking system, which is comprised of a silicon microstrip tracker (SMT) and a central fiber tracker (CFT), both located within a 2 T superconducting solenoidal magnet [3]. The muon momenta are measured from the curvature of the muon tracks in the central-tracking system. Jets are reconstructed from energy depositions in the three liquid-argon/uranium calorimeters: a central section (CC) covering $|\eta|$ up to ≈ 1 , and two end calorimeters (EC) extending coverage to $|\eta| \approx 4$, all housed in separate cryostats [4]. Scintillators between the CC and EC cryostats provide sampling of developing showers at $1.1 < |\eta| < 1.4$. A muon system resides beyond the calorimetry, and consists of a layer of proportional-wire tracking detectors and scintillation trigger counters before 1.8 T toroids, followed by two more similar layers after the toroids. The muon system is used for triggering and identifying muons.

The data used in this analysis were collected between August 2002 and July 2003. The integrated luminosity is $(294 \pm 19) \text{ pb}^{-1}$. Only events which pass a combination of single- or di-muon triggers were considered. At the first trigger level, a muon was triggered by a coincidence of hits in at least two of the three scintillator layers of the muon system within a time window consistent with muons coming from the interaction point. At the second trigger level, a muon track was identified from the hits in the drift-tube detectors and the scintillators of the muon system, allowing the rejection of low-momentum muons. Events passing the single- or di-muon triggers at first level were then required to have a second muon in the events or a track in the central-tracking system above a p_T threshold needed to be identified at level 2 or 3 of the $D\bar{O}$ trigger system. The efficiency of the trigger combination for $\mu j + \mu j$ events was measured with data.

Muons in the region $|\eta| < 1.9$ were reconstructed from hits in the three layers of the muon system which could be identified with isolated tracks in the central-tracking system. Cosmic muon events were rejected by cuts on the timing in the muon scintillators and by removing back-to-back muons. Jets are reconstructed using the iterative, midpoint cone algorithm [5] with a cone size of 0.5. The jet energies were calibrated as a function of the jet transverse energy and η by balancing energy in photon plus jet events. Only jets which were well contained within the detector were considered by requiring $|\eta| < 2.4$.

Due to the isolation requirement and the excellent shielding of the muon detectors, the background is dominated by Z -Boson/Drell-Yan (Z/DY) $Z/\gamma^* \rightarrow \mu\mu$ (+jets) events. To evaluate the contribution from Z/DY background, samples of Monte Carlo (MC) events were generated with PYTHIA [6]. Additional ALPGEN [7] samples were generated to estimate the uncertainty of the jet transverse energy shape. Additional samples of PYTHIA $t\bar{t}$ ($m_t = 175 \text{ GeV}$) and PYTHIA WW samples were used to estimate the background contributions from top quark and W pair processes, respectively. The signal efficiencies were calculated using PYTHIA samples of $LQ_2\bar{L}Q_2 \rightarrow \mu j \mu j$ Monte Carlo events for leptoquark masses from 140 to 300 GeV in steps of 20 GeV. All Monte Carlo events were processed using a full simulation of the $D\bar{O}$ detector based on GEANT [8] and the event reconstruction. Differences in the trigger and reconstruction efficiencies between data and Monte Carlo were taken into account using proper weightings of the MC events.

This analysis required two muons with transverse momentum exceeding $p_T = 15 \text{ GeV}$ and two jets with transverse energy (E_T) greater than 25 GeV. In order to reduce Z/DY background at high di-muon masses due to badly reconstructed muon tracks, the muon momentum was corrected taking advantage of the fact that no or little missing transverse energy is expected in both signal and Z/DY events. The missing transverse energy was approximated from the energy balance of all muons and jets ($E_T > 20 \text{ GeV}$) in the event and the momentum of the muon opposite to the direction of the missing transverse energy in the r - ϕ plane was corrected such that the missing transverse energy parallel to the muon vanished. The resulting degraded resolution and the shift to lower values of the di-muon mass in both data and MC due to this correction was outweighed by the suppression of badly reconstructed Z events in the high mass region where the search for leptoquarks took place. To further reduce the background from Z/DY events a Z -veto cut ($m(\mu\mu) > 105 \text{ GeV}$) is applied. Six events survive this last cut while $6.7 \pm 0.7(\text{stat.}) \pm 1.8(\text{syst.})$ are expected from standard model background, which is comprised of Drell-Yan Z +jets (6.0), top-antitop (0.7), and W pair (0.01) events.

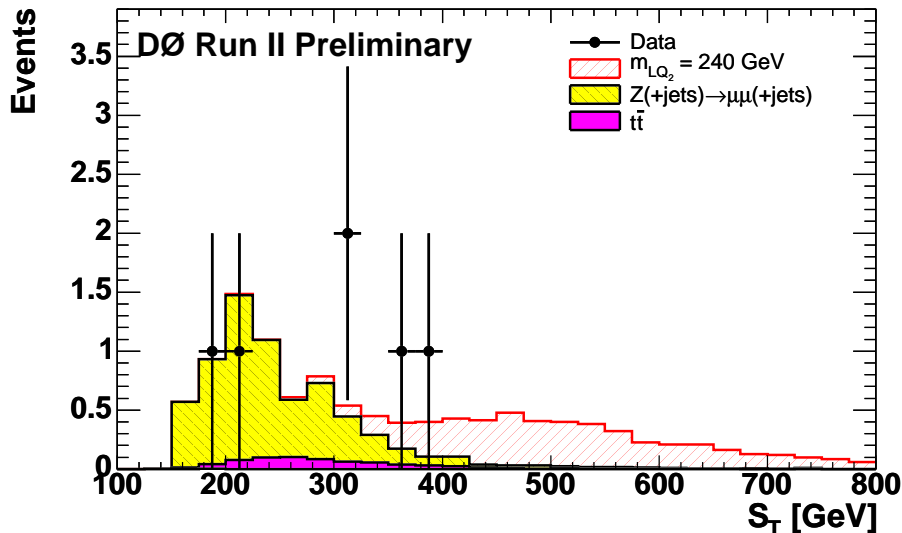


FIG. 1: Scalar sum of the transverse energies of the two highest- p_T muons and the two highest- E_T jets after the Z -veto cut.

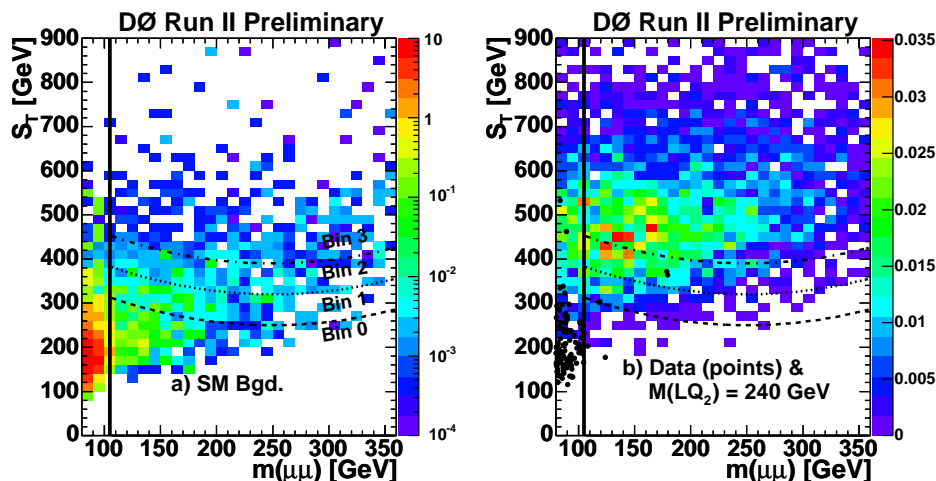


FIG. 2: Scalar sum of the transverse energies, S_T , as a function of the di-muon mass: a) for SM background; b) for data (black data points) and leptptoquark signal with a mass of $m_{LQ_2} = 240$ GeV. The vertical line illustrates the Z -veto cut and the curved lines show the edges of the signal bins (see text for definition).

$LQ_2\overline{LQ}_2 \rightarrow \mu j\mu j$ events are expected to have both high di-muon masses and large values of S_T which is the scalar sum of the transverse energies of the $\mu j\mu j$ system (see Fig. 1).

The remaining events after the Z -veto cut were arranged in four bins, from bin 0 to bin 3. The cut for bin i ($i \in \{1, 2, 3\}$) is defined as:

$$S_T > 0.003 \cdot (m(\mu\mu) - 250 \text{ GeV})^2 + 180 \text{ GeV} + i \cdot 70 \text{ GeV},$$

where $m(\mu\mu)$ is the invariant di-muon mass. Since each event is allowed to contribute only once, the event is assigned to the highest possible bin for which it passes the corresponding cut. The remaining events with the lowest signal over background ratio end up in the first bin, i.e. bin 0. The binning of the remaining events is illustrated by the curved lines in Fig. 2 at the example of second-generation leptptoquarks with a mass of 240 GeV.

The distribution of the four signal bins is shown in Fig. 3. Table I summarizes the efficiency for two leptptoquarks mass points as well as the number of expected background events and the distribution of the data into the four signal bins.

The dominant errors on the predicted number of background events are Monte Carlo statistics, varying between 7 and 25% for the four signal bins. The jet-energy scale error (2 - 12%) and the jet-energy shape error in Drell-Yan Z events (20%), which has been estimated by a comparison of the PYTHIA [6] simulation with Monte Carlo events

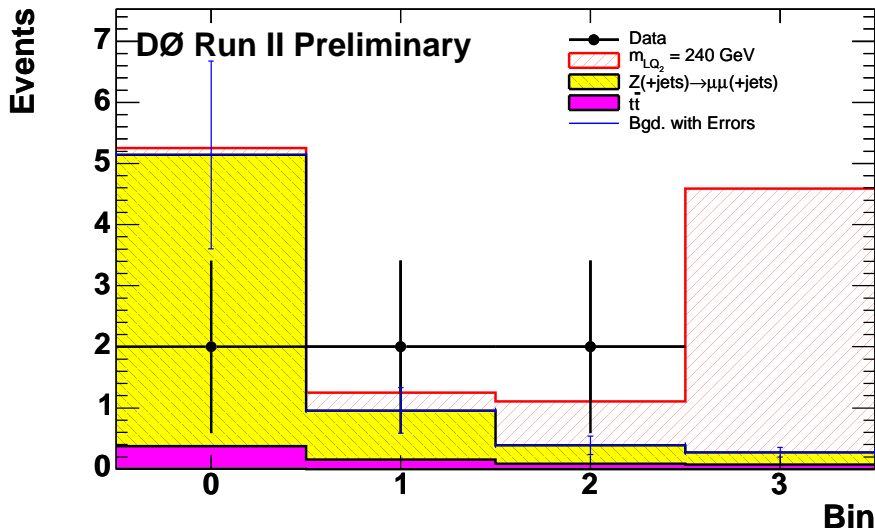


FIG. 3: Distribution of events over the four signal bins as defined in the text for a scalar leptoquark mass of $M_{LQ_2} = 240$ GeV.

TABLE I: Signal efficiency (ε) for $\beta = 1$, number of expected background events ($N_{\text{pred}}^{\text{bgd}}$), and the number of data events (N_{data}). The first error is the error due to limited Monte Carlo statistics, the second denotes the systematic uncertainty.

Cut	$\varepsilon(m_{LQ_2} = 200 \text{ GeV})$	$\varepsilon(m_{LQ_2} = 240 \text{ GeV})$	$N_{\text{pred}}^{\text{bgd}}$	N_{data}
$m(\mu\mu) > 105 \text{ GeV}$	$0.215 \pm 0.006 \pm 0.018$	$0.243 \pm 0.004 \pm 0.021$	$6.76 \pm 0.73 \pm 1.86$	6
Bin 0	$0.009 \pm 0.001 \pm 0.001$	$0.005 \pm 0.001 \pm 0.000$	$5.14 \pm 0.68 \pm 1.41$	2
Bin 1	$0.026 \pm 0.002 \pm 0.003$	$0.013 \pm 0.001 \pm 0.002$	$0.96 \pm 0.24 \pm 0.28$	2
Bin 2	$0.047 \pm 0.003 \pm 0.004$	$0.032 \pm 0.002 \pm 0.003$	$0.39 \pm 0.10 \pm 0.11$	2
Bin 3	$0.133 \pm 0.005 \pm 0.014$	$0.193 \pm 0.004 \pm 0.018$	$0.27 \pm 0.02 \pm 0.08$	0

generated with the ALPGEN [7] event generator, are the second largest sources of systematic uncertainty. The jet-multiplicity in the leading-order Monte Carlo generation (PYTHIA) of Drell-Yan $Z \rightarrow \mu\mu$ events was corrected in order to reflect the Berends' scaling in the data around the Z -resonance. This was done by a comparison of exponential fits to the inclusive jet multiplicities in data and Monte Carlo. The remaining difference between $\mu\mu + jj$ events the data and the PYTHIA Monte Carlo in the vicinity of the Z resonance, $60 \text{ GeV} < m(\mu\mu) < 105 \text{ GeV}$, was taken as the corresponding systematic uncertainty (16%). In addition, the following sources of systematic errors were taken into account: luminosity (6.5%), theoretical cross section of the DY/ Z processes (3.6%), and muon triggering and identification (5%). The systematic errors, added in quadrature, are shown in Tab. I.

The systematic errors of the signal efficiencies arise from limited Monte Carlo statistics (2 - 17%), jet-energy scale (3 - 13%), muon triggering and identification (3.3%), and PDF uncertainty (2%).

No significant excess of data over background was found. Therefore, assuming a branching fraction to charged leptons of $\beta = \text{Bf}(LQ_2 \rightarrow \mu j) = 1$, the upper limit on the cross section, $\sigma_{\text{obs}}^{95\% \text{ C.L.}}$, was calculated. This calculation was performed assuming a flat prior and Gaussian errors as described in reference [9] with the correlations of systematic errors taken into account (both between different channels/bins, as well as between the signal acceptance, the background prediction and the luminosity). The observed limit is calculated using the confidence level $CL_S = CL_{S+B}/CL_B$, where CL_{S+B} is the confidence level for the signal plus background hypothesis and CL_B is the confidence level for the background only. The cross section limits and the theoretical predictions [10] are shown in Fig. 4 and Tab. II. The mass limit is extracted from the intersection of the lower edge of the NLO cross section error band with the observed upper bound to the cross section. The error band contains the PDF error [11] as well as the variation of the factorization and normalization scale between $M_{LQ}/2$ and $2M_{LQ}$, added in quadrature.

The branching fraction for the process $LQ_2 \bar{L}Q_2 \rightarrow \mu j + \mu j$ is $\beta^2 = \text{Bf}(LQ_2 \rightarrow \mu j)^2$. Figure 5 shows the excluded region in the β versus m_{LQ_2} parameter space. The lower limit to the mass of scalar second generation leptoquarks was determined to $m_{LQ_2} > 247 \text{ GeV}$ and $m_{LQ_2} > 182 \text{ GeV}$ for $\beta = 1$ and $\beta = 1/2$, respectively. The corresponding expected limits, calculated from Monte Carlo events only, are $m_{LQ_2}^{\text{expected}} > 251 \text{ GeV}$ and $m_{LQ_2}^{\text{expected}} > 199 \text{ GeV}$.

A similar analysis in the $\mu j + \mu j$ channel was performed with the DØ Run I data [12] using $(94 \pm 5) \text{ pb}^{-1}$ at

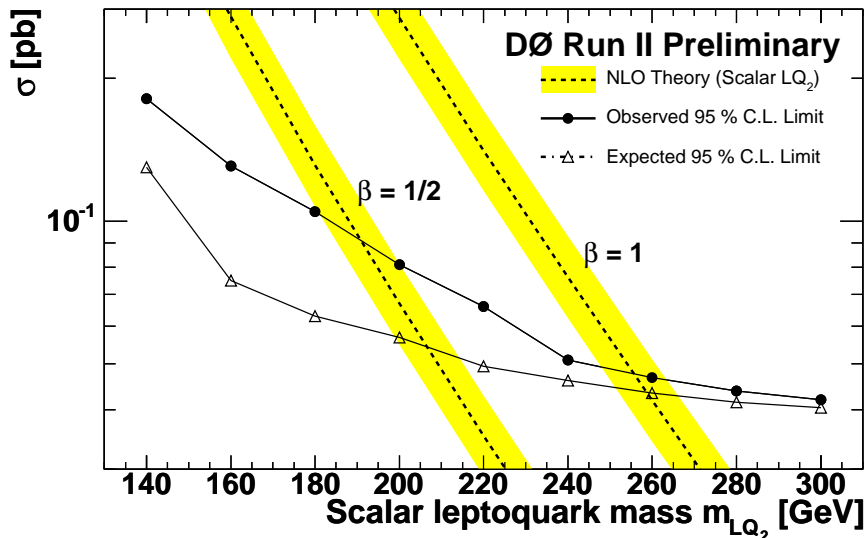


FIG. 4: Calculated cross sections for scalar second-generation leptoquarks for $\beta = 1$ and $\beta = 1/2$ as compared to the 95 % C.L. upper limit on the cross section. The leading-order (LO) cross section is taken from PYTHIA. The error band for the next-to-leading-order (NLO) cross section [10] originates from a variation of the renormalisation and factorisation scale between $m_{LQ}/2$ and $2m_{LQ}$ and the PDF errors, added in quadrature.

TABLE II: Efficiencies and NLO cross sections for scalar leptoquark pair production at Run I and II, 95 % C.L. upper cross section limits for the analysis described in this document, and the results from the Run I + Run II combination. The cross sections shown are calculated using CTEQ6.1M as PDF [11] and m_{LQ} as the factorization/normalization scale [10].

Leptoquark mass $m_{LQ_2} [GeV]$	ϵ , Run I $\mu j + \mu j$	ϵ , Run I $\mu j + \nu j$	$\sigma_{\text{theory}}^{\text{Run I}}$ $\sqrt{s} = 1.8 \text{ TeV}$	$\sigma_{\text{theory}}^{\text{Run II}}$ $\sqrt{s} = 1.96 \text{ TeV}$	Run II $\sigma_{\text{obs.}}^{95\% \text{ C.L.}}$ $\sqrt{s} = 1.96 \text{ TeV}$	Run I + II $\sigma_{\text{obs.}}^{95\% \text{ C.L.}}$ $\sqrt{s} = 1.96 \text{ TeV}$
140	0.103 ± 0.011	0.072 ± 0.011	1.8 pb	$2.380^{+0.487}_{-0.448}$ pb	0.181 pb	0.144 pb
160	0.145 ± 0.016	0.103 ± 0.015	0.8 pb	$1.080^{+0.225}_{-0.200}$ pb	0.131 pb	0.104 pb
180	0.189 ± 0.021	0.122 ± 0.018	0.379 pb	$0.525^{+0.111}_{-0.096}$ pb	0.105 pb	0.083 pb
200	0.218 ± 0.021	0.134 ± 0.020	0.188 pb	$0.268^{+0.057}_{-0.049}$ pb	0.081 pb	0.064 pb
220	0.226 ± 0.024	0.141 ± 0.021	0.0958 pb	$0.141^{+0.030}_{-0.025}$ pb	0.066 pb	0.052 pb
240	0.235 ± 0.025	0.152 ± 0.023	0.0499 pb	$0.076^{+0.017}_{-0.015}$ pb	0.051 pb	0.045 pb
260	0.243 ± 0.026	0.155 ± 0.023	0.0265 pb	$0.042^{+0.009}_{-0.008}$ pb	0.047 pb	0.042 pb
280	0.260 ± 0.028	0.163 ± 0.024	0.0142 pb	$0.023^{+0.005}_{-0.004}$ pb	0.044 pb	0.038 pb
300	0.253 ± 0.028	0.157 ± 0.023	0.0076 pb	$0.013^{+0.003}_{-0.002}$ pb	0.042 pb	0.037 pb

$\sqrt{s} = 1.8 \text{ TeV}$. After all cuts, zero events were left in the data while 0.7 ± 0.5 were expected from the background. Another Run I analysis in the $\mu j + \nu j$ channel yielded zero events for 0.7 ± 0.9 events expected from standard model background [12]. The branching fraction for this channel is $\text{Bf}(LQ_2 \overline{LQ}_2 \rightarrow \mu j + \nu j) = 2\beta(1 - \beta)$. Taking into account the smaller cross section for scalar leptoquark production at the Run I centre-of-mass energy $\sqrt{s} = 1.8 \text{ TeV}$, these earlier results have been combined with the Run II analysis presented in this document. The results are summarized in Tab. II and the excluded parameter regions are shown in Fig. 5. The combined upper limit for scalar leptoquarks of the second generation is $m_{LQ_2} > 251 \text{ GeV}$ ($m_{LQ_2} > 204 \text{ GeV}$) for $\beta = 1$ ($\beta = 1/2$).

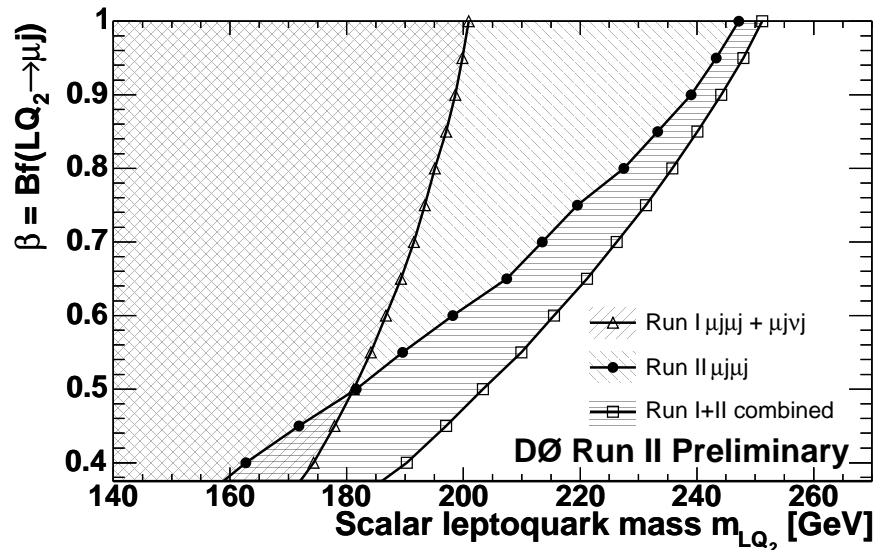


FIG. 5: Excluded parameter space for scalar second-generation leptoquarks at 95 % confidence level.

Acknowledgments

We thank the staffs at Fermilab and collaborating institutions, and acknowledge support from the DOE and NSF (USA); CEA and CNRS/IN2P3 (France); FASI, Rosatom and RFBR (Russia); CAPES, CNPq, FAPERJ, FAPESP and FUNDUNESP (Brazil); DAE and DST (India); Colciencias (Colombia); CONACyT (Mexico); KRF (Korea); CONICET and UBACyT (Argentina); FOM (The Netherlands); PPARC (United Kingdom); MSMT (Czech Republic); CRC Program, CFI, NSERC and WestGrid Project (Canada); BMBF and DFG (Germany); SFI (Ireland); Research Corporation, Alexander von Humboldt Foundation, and the Marie Curie Program.

-
- [1] J.C Pati and A. Salam, Phys. Rev. D **10**, 275 (1974);
E. Eichten *et al.*, *ibid.* **34**, 1547 (1986);
W. Buchmüller and D. Wyler, Phys. Lett. B **177**, 377 (1986);
E. Eichten *et al.*, Phys. Rev. Lett. **50**, 811 (1983);
H. Georgi and S. Glashow, *ibid.* **32**, 438 (1974).
 - [2] M. Leurer, Phys. Rev. D **49**, 333 (1994).
 - [3] DØ Collaboration, V. Abazov *et al.*, “The Upgraded DØ Detector”, in preparation for submission to Nucl. Instrum. Methods Phys. Res. A, and T. LeCompte and H.T. Diehl, Ann. Rev. Nucl. Part. Sci. **50**, 71 (2000).
 - [4] DØ Collaboration, S. Abachi *et al.*, Nucl. Instrum. Methods Phys. Res. A **338**, 185 (1994).
 - [5] G. Blazey, et al., in Proceedings of the workshop “QCD and Weak Boson Physics in Run II”, edited by U. Baur, R.K. Ellis, and D. Zeppenfeld, Batavia, p. 47 (2000).
 - [6] T. Sjöstrand, Comput. Phys. Commun. **82**, 74 (1994).
 - [7] M.L. Mangano, M. Moretti, F. Piccinini, R. Pittau, A. Polosa, hep-ph/0206293, JHEP **0307**, 001 (2003).
 - [8] R. Brun and F. Carminati, CERN Program Library Long Writeup W5013 (1993).
 - [9] Tom Junk, NIM A**434**, 435-443 (1999).
 - [10] M. Krämer, T. Plehn, M. Spira, P.M. Zerwas, Phys. Rev. Lett. **79** 341 (1997).
 - [11] J. Pumplin, D. R. Stump, J. Huston, H. L. Lai, P. Nadolsky and W. K. Tung, JHEP **0207** 012 (2002).
 - [12] The DØ Collaboration, B. Abbott et al., Phys. Rev. Lett. **84**, 2088 (2000).